Thickening Process and Kinetics of Lamellar Crystals of a Low Molecular Weight Poly(ethylene oxide)

Xiong-Feng Tang, Xiao-Jin Wen, Xue-Mei Zhai, Nan Xia, and Wei Wang*

The Key Laboratory of Functional Polymer Materials of Ministry of Education and Institute of Polymer Chemistry, College of Chemistry, Nankai University, Tianjin 300071, China

Gerhard Wegner

Max-Planck-Institute for Polymer Research, Ackermannweg 10, Postfach 3148, D-55128, Mainz, Germany

Zhong-Hua Wu

Beijing Synchrotron Radiation Facility, Institute of High Energy Physics, Chinese Academy of Sciences, Beijing 100049, China

Received February 16, 2007
Revised Manuscript Received April 3, 2007

Introduction

In the past decades the investigations on the crystallization and crystalline structures and morphologies of crystalline polymers have been highly focused.[1] The findings have provided an opportunity to have in-depth understandings of the nature of long chain macromolecules. Lower molecular weight polymers normally show an integral chain fold, so lamellar crystal thickness is always an integral submultiple of the total chain length and a step function of crystallization temperature. Folded-chain (FC) lamellar crystals with different thicknesses correspond to different morphologically metastable states, and only extended-chain (EC) crystals are in the thermodynamically equilibrium state. Because crystalline macromolecules kinetically prefer to be folded several times to form FC lamellar crystals under the supercooling condition, thin FC crystals will be thickened to form thick FC crystals and finally EC crystals when annealed in a temperature below the melting temperature.[2−14] The lamellar thickening is in fact a typical transformation from a metastable state with a lower stability to another metastable state with higher stability and finally to the equilibrium state (EC crystals). Thermodynamic driving force is to minimize the surface free energy of the lamellar crystals.

Lower molecular weight poly(ethylene oxide)s (PEO) are an ideal system of studying the thickening process and mechanism. The previous studies have demonstrated that the lamellar thickness of lower molecular weight PEOs are a function of the crystallization temperature.[15,16] Most interesting is a thickness jump at a critical crystallization temperature due to the different integral chain folds. Time-resolved small-angle X-ray scattering (SAXS) has been applied to perform in-situ observations of the thickening process, and the effects of molecular weight, end groups, and molecular architectures have been studied.[9] In our previous works, we have reported the spontaneous and inductive thickenings of lamellar crystal monolayers of a low molecular weight PEO fraction ($\bar{M}_n = 5000$ g/mol) on silicon wafer surface measured by atomic force microscopy (AFM).[14] In those works we have demonstrated that some parts of thin crystals could be spontaneously thickened via sliding motion to result in the formation of thick crystals which could further inductively thicken other thin crystals around via melting−recrystallization. The average thickness of crystals increases in a quantized manner with increasing temperature. In this work we will report our new findings of thickening kinetics of the bulk samples of the same PEO. The thickening process from once FC crystals to EC crystals in the iso- and nonthermal conditions was tracked using a quasi-time-resolved SAXS. Our focus will be placed on the thickening kinetics from once FC to EC crystals occurring in a narrow temperature regime below the melting point. Our finding shows that this thickening process can be well described by an exponential, different from the crystallization from melt.

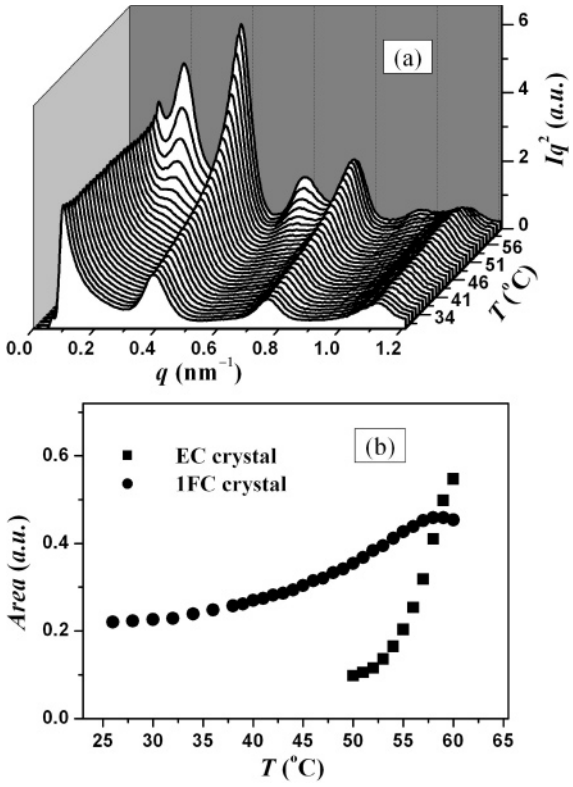

Figure 1. (a) Lorentz-corrected SAXS intensity profiles of a sample during the heating process from 26 to 60 °C. The recording time is 1800 s for each profile. (b) Temperature dependences of the integrated SAXS intensities of the first-order peaks of 1FC and EC crystals.

Results and Discussion

Lamellar Thickening during Heating Process. Figure 1a shows the SAXS profiles of a sample when was heated from 26 to 60 °C. The recording time for each profile is 1800 s. The long periods were determined from the position of peak maxima, and they change with the temperature (see Figure S1 in the Supporting Information). At $T \leq 49$ °C the SAXS profiles have three peaks, and their long periods are 16.0, 8.2, and 5.6 nm. The 1:2:3 ratios mean again that the 16.0 nm lamellae are the dominated structure. At $50 \leq T \leq 60$ °C the scattering intensity of the peak at $q = 0.39$ nm^{-1} starts to rapidly increase, meaning a growth of the 16.0 nm lamellar structure. Most interesting is the appearance and growth of three new peaks at $q = 0.19$, 0.59, and 1.00 nm^{-1}, respectively, indicating the formation of

* To whom correspondence should be addressed. E-mail: weiwang@nankai.edu.cn.

10.1021/ma070414d CCC: $37.00
Published on Web 05/09/2007

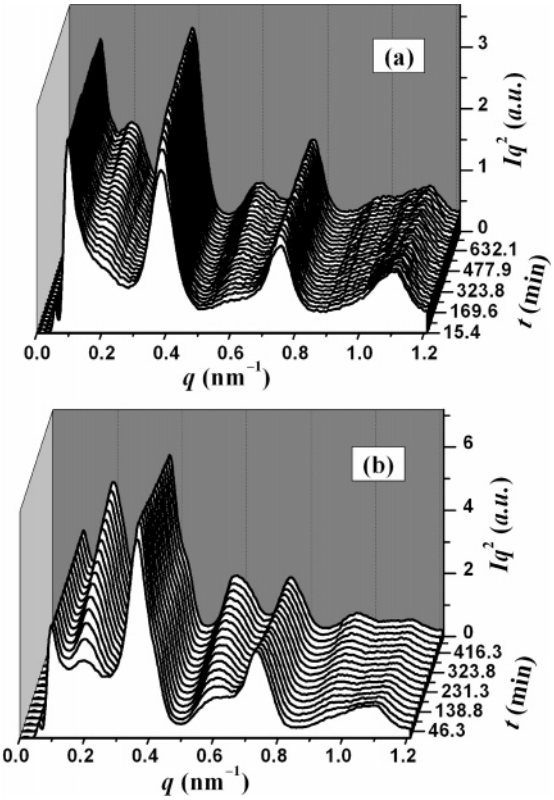

Figure 2. Time evolution of Lorentz-corrected SAXS intensity profiles for the samples annealed at 55 °C (a) and 58 °C (b).

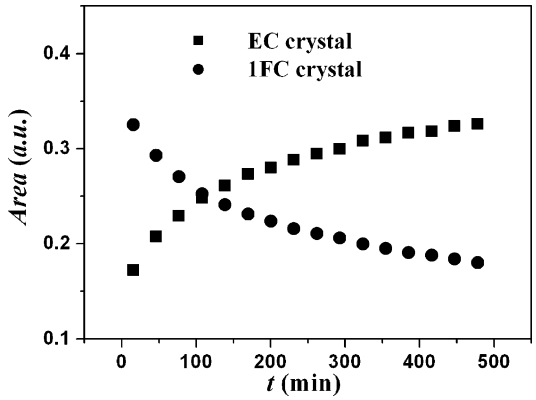

Figure 3. Time dependences of the integrated SAXS intensities of the first-order peaks of 1FC and EC crystals at 58 °C.

new and thick lamellar structure(s). The long periods of these peaks are 33.2, 16.0, 10.6, 8.3, 6.3, and 5.6 nm. Their ratios are approximately 1:2:3:4:5:6.

Figure 1b shows the temperature dependence of the integrated intensities of EC and 1FC.[17] At T < 55 °C the integrated intensity of 1FC crystals grows. EC crystals start to form at T = 49 °C, and its integrated intensity grows rapidly until 60 °C. The intensity increases of 1FC and EC crystals may be due to the crystallization of noncrystalline molecules.

Lamellar Thickening at Constant Annealing Temperatures. The further SAXS experiments were performed at 54 ≤ T ≤ 58 °C to monitor the formation of the EC crystals. Figure 2 shows the two sets of SAXS profiles obtained at T = 55 and 58 °C. (The data obtained at T = 54, 56, and 57 °C can be found in Figure S2 in the Supporting Information.) There are six scattering peaks in overall annealing process. The long periods are 31.9, 16.3, 10.5, 8.5, 6.3, and 5.7 nm at T = 58 °C. These long periods remain constant in the time regime covered

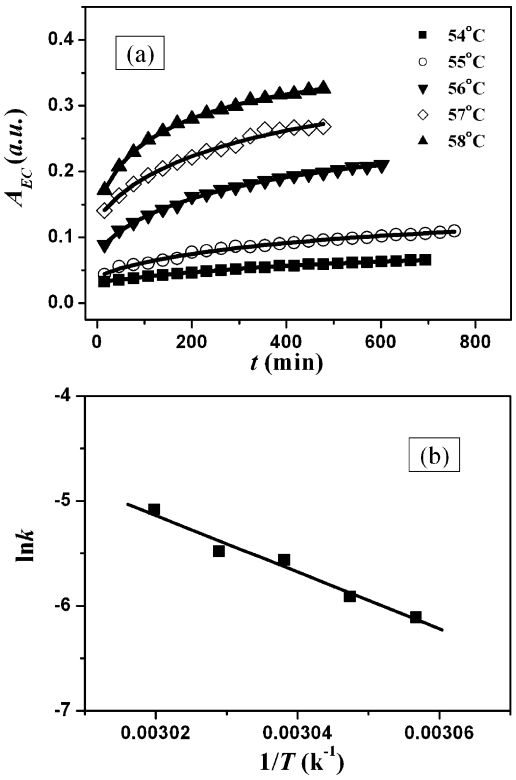

Figure 4. (a) Time dependences of the integrated SAXS intensity of extended chain lamellae at different annealing temperatures. The solid curves are the fitting results using eq 2. (b) Arrhenius plot of the rate constants and inversed absolute temperature. The activation energy is 224.4 ± 22.4 kJ/mol.

in this experiment (see Figure S3 in the Supporting Information). In Figure 2 the intensity increase of the first peak with a 31.9 nm long period indicates the formation and growth of EC crystals with increasing annealing time. Its intensity increase also results in the relative changes of other scattering peaks at a certain extent.

Figure 3 illustrates the integrated intensities as a function of the annealing time at T = 58 °C. The integrated intensity of EC crystals grows but that of 1FC crystals decays. Those can indicate that EC crystals form and then grow while 1FC crystals melt.

Thickening Kinetics. To study the kinetics of thickening process during isothermal annealing, a quantitative analysis of the scattering intensity curves was carried out by the least-square fitting. The measured scattering intensities, $I_1(q) = I(q)q^2$, are fitted well using the Lorentzian function for the crystalline peaks and the exponential decay function for background scattering:

$$I_1(q) = A_n \exp\left(\frac{q}{t_n}\right) + \sum_i \frac{2A_i}{\pi} \frac{W_i}{4(q - x_c)^2 + W_i^2} \qquad (1)$$

where A_n and t_n are the parameters of background scattering, A_i and W_i are the areas and full widths at half-maximum, and x_c is the position of peak maximum.

The fitting result meets the experimental curve very well (see Figure S4 in the Supporting Information). The areas, A_{EC} and A_{1FC}, under the EC and 1FC scattering peaks are the integrated scattering intensities, I_{EC} and I_{1FC}, which are proportional to the contents of these crystals. Figure 4a displays $A_{EC} \sim t$ curves obtained at different annealing temperatures. The relation between A_{EC} and t can be well described by an exponential equation:

$$A_{EC}(T,t) = A(T,t=0) + \exp(-k(T)t) \qquad (2)$$

where $A(T,t=0)$ is the peak area at $t = 0$ and $k(T)$ is a rate constant. According to Arrhenius theory, the rate constant $k(T)$ is a function of temperature

$$k(T) = k_0 \exp(-\Delta E/RT) \quad (3)$$

where k_0 is the temperature-independent preexponential factor, ΔE is an activation energy, and R and T are the gas constant and the absolute temperature, respectively. The least-squares linear regression of data of ln k against $1/T$ determines $\Delta E/R$ (see Figure 4b). The activation energy, ΔE, is found to be 224.4 $\pm$ 22.4 kJ/mol for the EC crystal formation.

Thickening Mechanism. The thickening observed is a typical Ostwald ripining[18] of lamellar crystals. Thermodynamic driving force of the thickening is naturally to minimize the surface free energy of the lamellar crystals. The high free energy of folded-chain surface caused by chain folds dominates the total free energy, so minimization of the free energy of folded-chain surface becomes the key driving force of the thickening of lamellar crystals. Because the low molecular weight PEOs prefer integral chain folds to avoid defects of chain-end groups forming within the lamellar crystals, the thickening is in a quantized manner.

There are two main mechanisms that have been proposed to explain the thickening process. One of them is the sliding motion mechanism in which molecules in thinner lamellae are suggested to migrate to adjacent lamellae through an amorphous layer via sliding motion along the crystallographic c-axis.[3,6,7,9−11,14] According to this mechanism, the thickness of the thickened lamellae is normally doubled. Melting−recrystallization is another important mechanism which emphasizes melting of thinner lamellae and recrystallization into thicker lamellae.[2,4,7,8,14] In fact, these mechanisms clearly involve three important steps as follows: The molecules leave or melt from thinner crystals (the ordered but less metastable state). They enter and then diffuse through the amorphous phase (disordered state) toward thicker crystals. Finally, they enter or are absorbed by and recrystallize in the thicker crystals (ordered and more metastable or finally equilibrium state). The most difficult step of the three will determine the entire thickening process.

In Figure 4a we have demonstrated that thickening process can be well described by an exponential (see eq 2). It is interesting to mention that this equation is totally the same as that used to describe the center-of-mass diffusion. If the diffusion through the amorphous phase was the key step, the mechanism of controlling the entire thickening process might be a linear chain motion. The high activation energy (224.4 $\pm$ 22.4 kJ/mol) also reflects the motion difficulty of the long chain macromolecules. Possibly, it is a cooperation process in which a number of molecules move simultaneously.

Conclusion

In this work we have used quasi-time-resolved SAXS to investigate the thickening process and kinetics of a PEO with a molecular weight $\bar{M}_n = 5000$ g/mol. In the initial samples once-folded lamellar crystals are the dominate structure. When they were heated to 50 °C, the once-folded chain lamellae started to melt and then gradually formed extended-chain (EC) crystals. The growth kinetics of EC crystals, obtained in isothermal experiments at $54 \leq T \leq 58$ °C, show that the thickening kinetics might be controlled by a center-of-mass diffusion with an activation energy of 224.4 $\pm$ 22.4 kJ/mol. The suggested mechanism is as follows: The molecules melted from thinner crystals (the ordered but less metastable state) first enter the amorphous phase (disordered state). Then they diffuse through the amorphous phase toward the thicker crystals and finally are absorbed by and recrystallize in the thicker crystals (ordered and more metastable or finally equilibrium state).

Acknowledgment. The Nankai group very greatly appreciates Nankai University for a start-up funding and National Science Foundation of China for a grant (NSFC20474033) to support this work. W.W. thanks Deutscher Akademischer Austausch Dienst (DAAD A/04/12961) for a scholarship which supported him in completing most SAXS experiments in Max-Planck-Institute for Polymer Research. The Nankai group thanks Beijing Synchrotron Radiation Facility (BSRF) at Institute of High Energy Physics of Chinese Academy of Sciences for a special grant to perform the initial SAXS experiments in the SAXS station of BSRF. Finally, we greatly appreciate Professor Stephen Z. D. Cheng for valuable discussions.

Supporting Information Available: Experimental details, SAXS data obtained at $T = 54$, 56, and 57 °C, and the long periods as a function of temperature or time. This material is available free of charge via the Internet at http://pubs.acs.org.

References and Notes

(1) (a) Wunderlich, B. *Macromolecular Physics*; Academic: New York, 1976; Vols. 1 and 2. (b) Armistead, K.; Goldbeck-Wood, G. *Adv. Polym. Sci.* **1992**, *100*, 219. (c) Schultz, J. M. *Polymer Crystallization. The Development of Crystalline Order in Thermoplastic Polymers*; Oxford University Press: Oxford, 2001. (d) Ungar, G.; Zeng, X.-B. *Chem. Rev.* **2001**, *101*, 4157. (e) Strobl, G. *Prog. Polym. Sci.* **2006**, *31*, 398. (e) Keller, A.; Cheng, S. Z. D. *Polymer* **1998**, *39*, 4461.
(2) Mandelkern, L.; Sharma, R. K.; Jackson, J. F. *Macromolecules* **1969**, *2*, 644.
(3) Dreyfuss, P.; Keller, A. *J. Macromol. Sci., Phys.* **1970**, *B4*, 811.
(4) Fischer, E. W. *Pure Appl. Chem.* **1971**, *26*, 385.
(5) (a) Kovacs, A. J.; Gonthier, A. *Colloid Polym. Sci.* **1972**, *250*, 530. (b) Kovacs, A.; Gonthier, A.; Straupe, C. *J. Polym. Sci., Polym. Symp.* **1975**, *50*, 283. (c) Kovacs. A.; Straupe, C.; Gonthier, A. *Polym. Sci., Polym. Symp.* **1977**, *59*, 31. (e) Kovacs, A. J.; Straupe, C. *Faraday Discuss. Chem. Soc.* **1979**, *68*, 225. (f) Kovacs, A.; Straupe, C. *J. Cryst. Growth* **1980**, *48*, 210.
(6) Ungar, G.; Steiny, J.; Keller, A.; Bidd, I.; Whitting, M. C. *Science* **1985**, *229*, 386.
(7) Ichida, T.; Tsuji, M.; Murakami, S.; Kawaguchi, A.; Katayama, K. *Colloid Polym. Sci.* **1985**, *263*, 293.
(8) Phillips, P. J.; Rensch, G. J. *J. Polym. Sci., Polym. Phys. Ed.* **1989**, *27*, 155.
(9) (a) Cheng, S. Z. D.; Zhang, A.-Q.; Barley, J. S.; Chen, J.-H.; Habenschuss, A.; Zschack, P. R. *Macromolecules* **1991**, *24*, 3937. (b) Cheng, S. Z. D.; Chen, J.-H.; Zhang, A.-Q.; Barley, J. S.; Habenschuss, A.; Zschack, P. R. *Macromolecules* **1992**, *25*, 1453. (c) Cheng, S. Z. D.; Wu, S. S.; Chen, J.-H.; Zhuo, Q.; Quirk, R. P.; von Meerwall, E. D.; Hsiao, B. S.; Habenschuss, A.; Zschack, P. R. *Macromolecules* **1993**, *26*, 5105. (d) Chen, E.-Q.; Lee, S. W.; Zhang, A.; Moon, B. S.; Harris, F. W.; Cheng, S. Z. D.; Hsiao, B. S.; Yeh, F.; Merrewell, E. V.; Grubb, D. T. *Macromolecules* **1999**, *32*, 4784.
(10) Yamamoto, T. *J. Chem. Phys.* **1997**, *107*, 2653.
(11) Rastogi, S.; Spoelstra, A. B.; Goossens, J. G. P.; Lemstra, P. J. *Macromolecules* **1997**, *30*, 7880.
(12) Liu, C.; Muthukumar, M. *J. Chem. Phys.* **1998**, *109*, 2563.
(13) Reiter, G.; Castelein, G.; Sommer, J.-U. *Phys. Rev. Lett.* **2001**, *86*, 5918.
(14) (a) Zhai, X. M.; Wang, W.; Ma, Z. P.; Wen, X. J.; Yuan, F.; Tang, X. F.; He, B. L. *Macromolecules* **2005**, *38*, 1717. (b) Zhai, X. M.; Zhang, G.-L.; Ma, Z. P.; Tang, X. F.; Wang, W. *Macromol. Chem. Phys.* **2007**, *208*, 651.
(15) Arlie, P.; Spegt, P. A.; Skoulios, A. *Makomol. Chem.* **1966**, *99*, 160; **1967**, *104*, 212.
(16) Spegt, P. *Makromol. Chem.* **1970**, *139*, 139.
(17) The peak area varies as n^{-2} where n is the peak order number. The area of the first order of 1FC peak was calculated by taking away the contribution of the second order of EC peak.
(18) Ostwald, W. *Z. Phys. Chem.* **1897**, *22*, 289.

MA070414D